ISSN 0208-7774 TRIBOLOGIA 2/2023 p. 35–44
DOI: 10.5604/01.3001.0053.6122

Joanna KOWALCZYK[*], Monika MADEJ[**], Dariusz OZIMINA[***]

EVALUATION OF THE EFFECTS OF ZDDP AND GRAPHENE ADDITIVES IN PAO 8 OIL ON THE TRIBOLOGICAL PROPERTIES OF TIALN COATING

OCENA WPŁYWU DODATKÓW ZDDP I GRAFENU W OLEJU PAO 8 NA WŁAŚCIWOŚCI TRIBOLOGICZNE POWŁOKI TiAlN

Key words: graphene, ZDDP, TiAlN coating, PAO 8, wear.

Abstract: This paper investigates the tribological effects of graphene and anti-wear zinc dialkyl dithiophosphates (ZDDP). Friction tests have been carried out on a tribological tester which operates as a ball and disc assembly in a frictional, sliding motion. Tests were carried out with a load of 10 N over a sliding distance of 1000 m. TiAlN coated HS6-5-2C steel discs, and 100Cr6 steel balls were used in the tests. Tests were conducted under lubrication conditions with poly(α)olefin oil PAO 8 with graphene and/or ZDDP. The chemical composition of the TiAlN coating was studied using a scanning electron microscope, and the wear marks on the discs and balls were observed. The geometric structure of the samples was analysed before and after the friction tests using a confocal microscope with interferometric mode. The results indicated that the addition of ZDDP and graphene to the poly(α)olefin oil had an effect on reducing the friction coefficient.

Słowa kluczowe: grafen, ZDDP, powłoka TiAlN, PAO 8, zużycie.

Streszczenie: W artykule określono wpływ grafenu i dodatku przeciwzużyciowego dialkiloditiofosforanu cynku ZDDP na właściwości tribologiczne. Badania tarciowe przeprowadzono na testerze tribologicznym pracującym w skojarzeniu trącym kula–tarcza w ruchu ślizgowym. Testy wykonano przy obciążeniu 10 N na drodze tarcia równej 1000 m. Do badań użyto tarcz ze stali HS6-5-2C z powłoką TiAlN oraz kul ze stali 100Cr6. Testy przeprowadzono w warunkach smarowania olejem poli(α)olefinowym PAO 8 z grafenem i/lub z ZDDP. Za pomocą mikroskopu skaningowego zbadano skład chemiczny powłoki TiAlN, a także obserwowano ślady wytarcia na tarczach i kulach. Przy użyciu mikroskopu konfokalnego z trybem interferometrycznym dokonano analizy struktury geometrycznej próbek przed oraz po testach tarciowych. Uzyskane wyniki badań wskazały, że dodatek ZDDP i grafenu do oleju poli(α)olefinowego wpłynął na zmniejszenie współczynnika tarcia.

INTRODUCTION

Physical Vapour Deposition (PVD) coatings are widely used for the improvement of material properties in a wide range of industrial applications **[L. 1]**. One of the most important characteristics of coatings applied by this method is good adhesion, high hardness, strength and controlled thickness **[L. 2]**. Among others, nitride-based coatings are produced using PVD technology. Due to their mechanical, wear, corrosion and other properties, nitride thin film coatings have a wide range of applications **[L. 3]**. TiN, TiCN and TiAlN coatings are currently in use on machine-cutting tools. TiN, TiAlN and TiCN coatings, on the other hand, are used in the industrial sector as multi-layer coatings for machine components. Over the past two decades, numerous studies have shown that high

[*] ORCID: 0000-0003-4641-0032. Kielce University of Technology, Tysiąclecia Państwa Polskiego 7 Ave., 25-314 Kielce, Poland.
[**] ORCID: 000-0001-9892-9181. Kielce University of Technology, Tysiąclecia Państwa Polskiego 7 Ave., 25-314 Kielce, Poland.
[***] ORCID: 0000-0001-5099-6342. Kielce University of Technology, Tysiąclecia Państwa Polskiego 7 Ave., 25-314 Kielce, Poland.

aluminium nitride coatings provide better wear protection at elevated operating temperatures than aluminium-free nitride coatings such as TiN. In addition, the main advantage of TiAlN is its thermal stability during dry processing at high temperatures of the order of 800°C **[L. 2, 3]**, higher hardness **[L. 4]**, resistance to oxidation **[L. 4, 5]** and lower thermal conductivity **[L. 4]**. In addition, at high temperatures and even in extremely aggressive aqueous environments, the TiAlN coating is resistant to wear and corrosion. The TiAlN coating has been used for the coating of 304 and 316L stainless steel substrates for the chemical and biomedical industries. The study's authors cited the pulp and paper, medical, moulding and automotive industries as having high corrosion resistance **[L. 4]**.

Aihua et al. **[L. 5]** compared the frictional properties of TiN, TiAlN, AlTiN and CrAlN coatings by physical evaporation from the gaseous phase with cathodic arc deposition CA-PVD. The results showed that the TiAlN coating had the best mechanical properties and the best wear resistance. Fox-Rabinovich et al. **[L. 6]** investigated the scratch and wear resistance of tools with TiAlN, AlTiN and AlCrN coatings at elevated temperatures up to 500°C. They found that the TiAlN coating had a longer service life, which has been linked to lower scratch resistance. One of the methods used to improve the bond strength, and therefore the mechanical and tribological properties, is the use of an intermediate layer.

In the present study, the tribological systems under investigation were lubricated with PAO polyalphaolefin oil with ZDDP zinc dialkyl dithiophosphates and graphene. The effect of these additives on the tribological properties of the systems under investigation has been the subject of analysis. PAO is a product of n-decene polymerisation. PAOs contain oligomers with an average degree of polymerisation between two and eight **[L. 7]**. Polyalphaolefins are characterised by exceptionally good viscosity-temperature properties, high thermal decomposition and ignition temperatures and low volatility. As a result, PAOs have long been among the most commonly used base oils **[L. 8]**. Synthetic oils have a number of significant advantages over mineral oils. For this reason, they are often used in extreme operating conditions. Additives that reduce friction and wear on the components of the tribological system are introduced to improve the properties of PAOs. One of these is zinc dialkyl dithiophosphates ZDDP. It is an anti-wear additive. It performs under a wide range of operating conditions when used in engine oils **[L. 7]**.

In recent years, carbon nanomaterials have attracted considerable interest due to their good lubricating properties. One example is flake graphene and its unique tribological properties due to this structure **[L. 9]**.

METHODOLOGY AND MATERIALS FOR TESTING

Tests were carried out using discs made from HS6-5-2C steel coated with TiAlN. The balls were made of 100Cr6 steel and had a diameter of 6 mm. HS6-5-2C steel HS6-5-2C is characterised by remarkably high ductility, impact strength and abrasion resistance. Its hardness after quenching and tempering at 550°C is 65 HRC **[L. 10]**. **Table 1** shows its chemical composition **[L. 11]**.

Table 1. Composition of HS6-5-2C steel [L. 11]
Tabela 1. Skład chemiczny stali HS6-5-2C **[L. 11]**

Element	%
C	0.82=0.92
Mn	≥ 0.40
Si	≥ 0.50
P	≥ 0.03
S	≥ 0.03
Cr	3.50=4.50
Ni	≥ 0.40
Mo	4.50=5.50
W	6=7
V	1.70=2.10
Co	≥ 0.50
Cu	≥ 0.30

Steel 100Cr6 is a high-carbon steel used for rolling elements, such as balls, rollers and runners. It is characterised by very good resistance to wear and fatigue – stability of elasticity and microstructure at high temperatures **[L. 12]**. Its chemical composition is summarised in **Table 2 [L. 13]**.

Table 2. Composition of 100Cr6 steel [L. 13]
Tabela 2. Skład chemiczny stali 100Cr6 **[L. 13]**

Element	%
C	0.93=1.05
Mn	0.25=0.45
Si	0.15=0.35
P	< 0.025
S	< 0.03
Cr	1.35=1.60
Cu	< 0.30

TiAlN coating was chosen based on its exceptionally good tribological properties, high hardness and resistance to oxidation. Because of these benefits, these coatings are used, for example, on cutting tools in the pulp and paper industry, in wood cutting processes, in the medical industry, in the moulding industry and also in the automotive industry for brake pads. **[L. 2, 4]**. The coating has been applied using the arc coating process at temperatures between 200–400°C. Its colour is purple-grey. According to the manufacturer's data, the TiAlN coating hardness was 33±3 GPa, the internal stress was approximately 0.6 GPa, and the coating thickness was 500µm **[L. 14]**.

Tribological tests were performed under PAO8 polyalphaolefin oil lubrication conditions. PAO 8 is a synthetic oil with a hydrocarbon structure (isoparaffins) produced by the catalytic oligomerisation of linear α-olefins. **Table 3** contains a list of the basic properties of PAO 8 oil.

Table 3. Properties of PAO 8
Tabela 3. Właściwości oleju PAO 8

Properties	Value
Specific gravity at 15.6°C	833 kg/m^3
Kinematic viscosity at 100°C 40°C -40°C	 7.8 mm^2/s 46.4 mm^2/s 19 570 mm^2/s
Viscosity Index	138

In the PAO 8 lubricant, the basic properties of which are given in **Table 4**, a 1.5% ZDDP additive was introduced.

Table 4. Properties of the commercial zinc dialkyl dithiophosphate (ZDDP) lubricant additive
Tabela 4. Podstawowe właściwości ZDDP

Properties	Value
Density (25°C)	1160 kg/m^3
Kinematic viscosity at 40°C	150 mm^2/s
Zn content	9.0% weight
P content	8.5% weight
S content	16.5% weight

In addition, graphene flakes with a low oxidation state, produced by Advanced Graphene Products, were also added to the PAO 8. Its main characteristics are shown in **Table 5**.

The lubricants used in the tribological tests were synthetic poly-alpha-olefin oil PAO 8, 1.5% (mass) ZDDP additive and graphene added at 0.005% (mass). After introducing eight additives to PAO: The ZDDP and the graphene were placed in an ultrasonic washing machine to ensure the components were thoroughly mixed.

Table 5. Properties of the graphene
Tabela 5. Podstawowe właściwości grafenu

Property	Value
Oxygen content	1–2%
Chemical composition–C	99.8%

Tribological tests were performed on a TRB^3 tribotester operating in a ball-disk frictional sliding motion. Tests were carried out with the following parameters:

- load P = 10 N,
- slip velocity v = 0.1 m/s,
- sliding distance s = 1000 m,
- friction pair: ball of 100Cr steel – disc of HS6-5-2C steel with TiAlN coating.
- lubricant: PAO 8, PAO 8 + ZDDP, PAO 8 + ZDDP + graphene.

Linear wear, coefficient of friction and wear mark area were analysed after the friction test. Wear marks on discs and balls were observed through a confocal microscope with Leica DCM8interferometric mode. However, the chemical composition of samples and counterexamples before and after tribological tests was analysed using a Phenom XL scanning electron microscope equipped with an EDS microanalyser. The chemical composition of the TiAlN coating used in the study was also analysed using a microscope.

RESEARCH RESULTS AND DISCUSSION

The chemical composition of the TiAlN coating is shown in **Figure 1**. The resulting analysis of the chemical composition shows that the dark areas are dominated by the share of titanium, later aluminium, followed by nitrogen and later the elements from the substrate. The name of this shell determines the order of the elements. Conversely, the bright area is a concentration of nitrogen, followed by aluminium, titanium and then substrate elements.

Wetting tests on the TiAlN-coated surfaces (**Fig. 2**) were performed with the lubricants used for tribological testing: PAO 8, PAO 8 + ZDDP, PAO 8 + ZDDP + graphene.

For all the lubricants tested, the values for the wetting angle were less than 90°, indicating that the

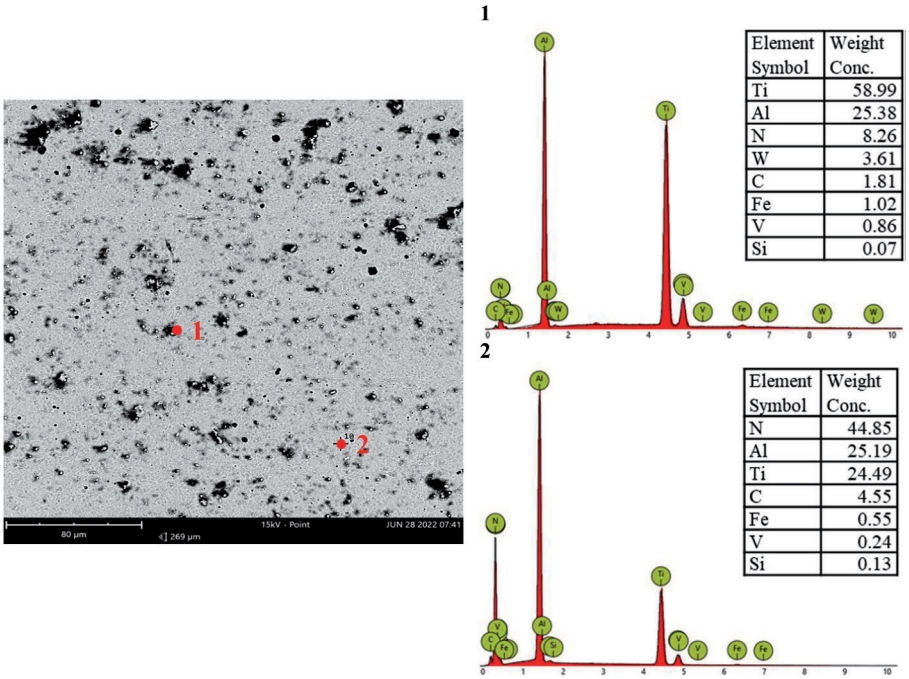

Fig. 1. X-ray spectrum of the TiAlN coating
Rys. 1. Widmo promieniowania rentgenowskiego powłoki TiAlN

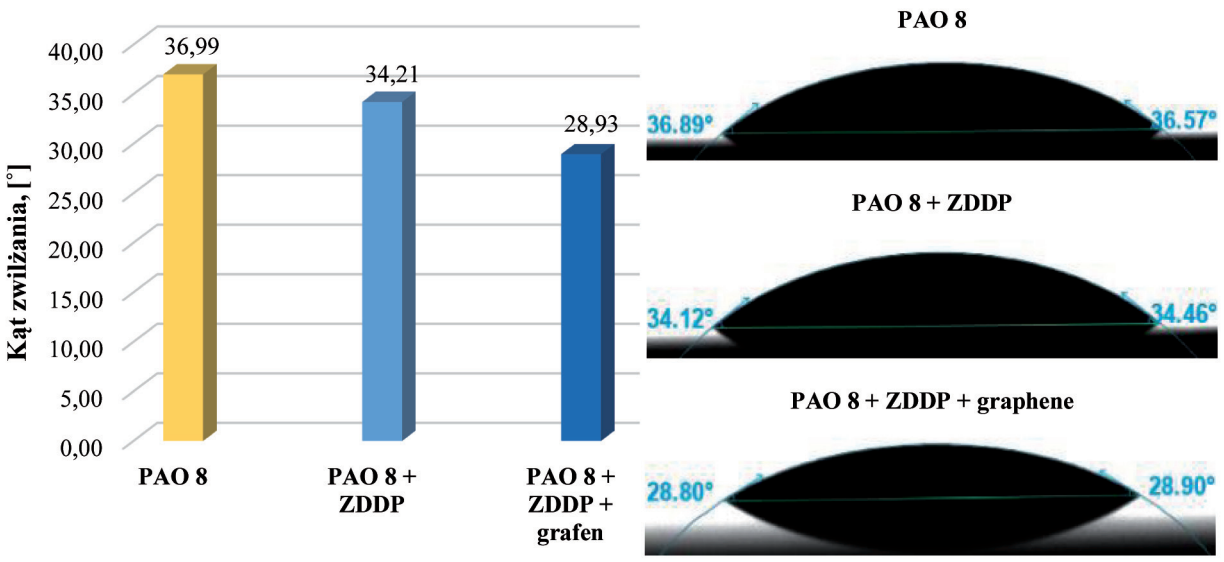

Fig. 2. Contact angles of surfaces with TiAlN coating with lubricants PAO 8, PAO 8 + ZDDP, PAO 8 + ZDDP + graphene
Rys. 2. Kąty zwilżania powierzchni z powłoką TiAlN substancjami smarującymi PAO 8, PAO 8 + ZDDP, PAO 8 + ZDDP + grafen

lubricants are wetting the surfaces. PAO 8 + ZDDP + graphene had the lowest and PAO 8 the highest wetting angle value.

Figure 3 summarises the graphs recorded during tribological testing as the mutual relationship: a) coefficients of friction and b) linear wear as a function of sliding distance.

In the analysis of the tribological results obtained, it was observed that the lowest value of the coefficient of friction was recorded under the PAO 8 + ZDDP + graphene lubrication condition and the highest value was recorded under the PAO 8 lubrication condition. The lowest value of the linear wear was recorded after the lubrication with the PAO 8 oil, and the highest value was after the friction with the PAO 8 + ZDDP + graphene lubrication.

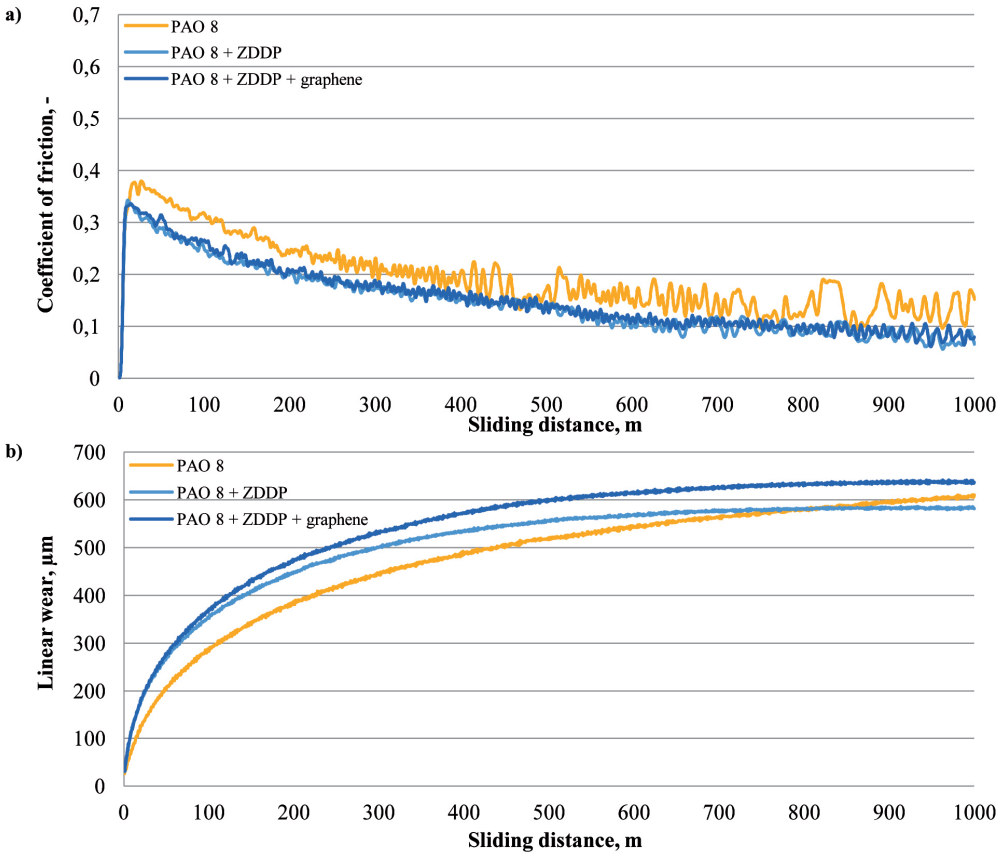

Fig. 3. The results of the tribological tests: a) coefficient of friction and b) linear wear
Rys. 3. Wyniki badań tribologicznych: a) współczynnik tarcia i b) zużycie liniowe

The use of a lubricant consisting of PAO 8 + ZDDP + graphene in friction tests reduced the friction coefficient by approximately 25% compared to PAO 8. PAO 8, on the other hand, helped to reduce wear by more than 6% compared to PAO 8 + ZDDP + graphene.

Before (**Fig. 4**) and after (**Fig. 5** and **Fig. 6**) the tribological tests, the discs and balls were observed using a confocal microscope under an interferometric mode of operation.

Figures 5 and **6** show isometric images and primary profiles of discs (**Figure 5**) and balls (**Figure 6**) after tribological tests under PAO 8, PAO 8 + ZDDP and PAO 8 + ZDDP + graphene lubrication conditions.

The formula (1 and 2) were used to calculate the wear of the balls after tribological tests under lubrication conditions with the test lubricants (**Table 6**):

$$V_{kuli} = \frac{1}{3}\pi h^2 (3R - h) \quad (1)$$

$$h = R - \sqrt{R^2 - r^2} \quad (2)$$

where:
r – radius of the wear mark,
h – height of area used,
R – radius of the ball.

Table 6. Worn balls after the tribological tests for PAO 8, PAO 8 + ZDDP and PAO 8 + ZDDP + graphene
Tabela 6. Zużycie kul po testach tribologicznych dla PAO 8, PAO 8 + ZDDP i PAO 8 + ZDDP + grafen

Radius and height of the worn ball / Lubricant	h [mm]	V [mm]
PAO 8	0.60	3.17
PAO 8 + ZDDP	0.59	3.02
PAO 8 + ZDDP + graphene	0.66	3.78

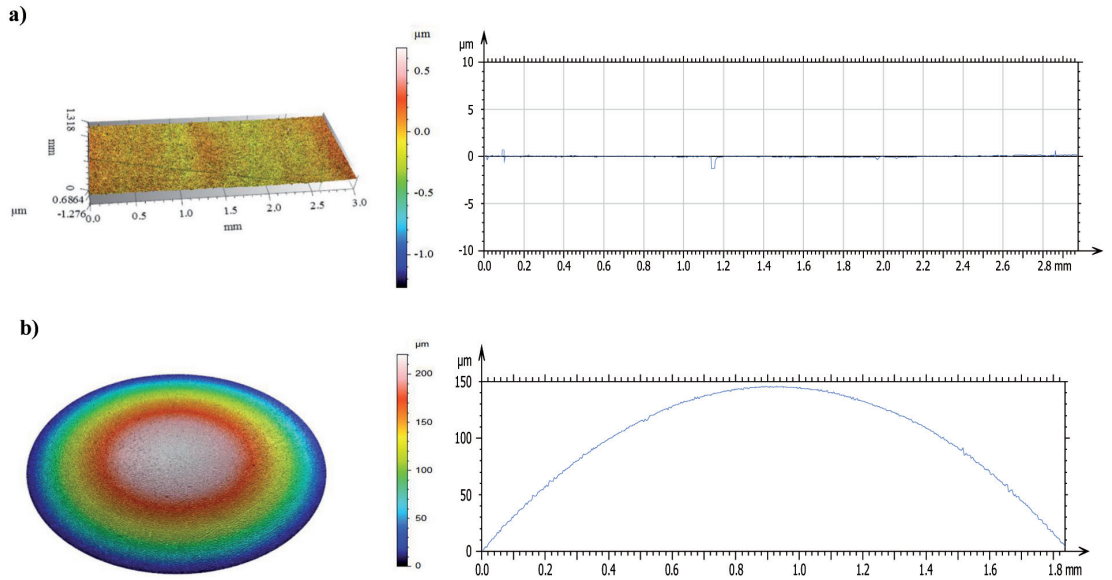

Fig. 4. Isometric views and primary profiles before the tribological tests of a) the steel disc with TiAlN coating, b) the steel ball

Rys. 4. Obrazy izometryczne i profile pierwotne przed badaniami tribologicznymi: a) stalowej tarczy z powłoką TiAlN, b) stalowej kuli

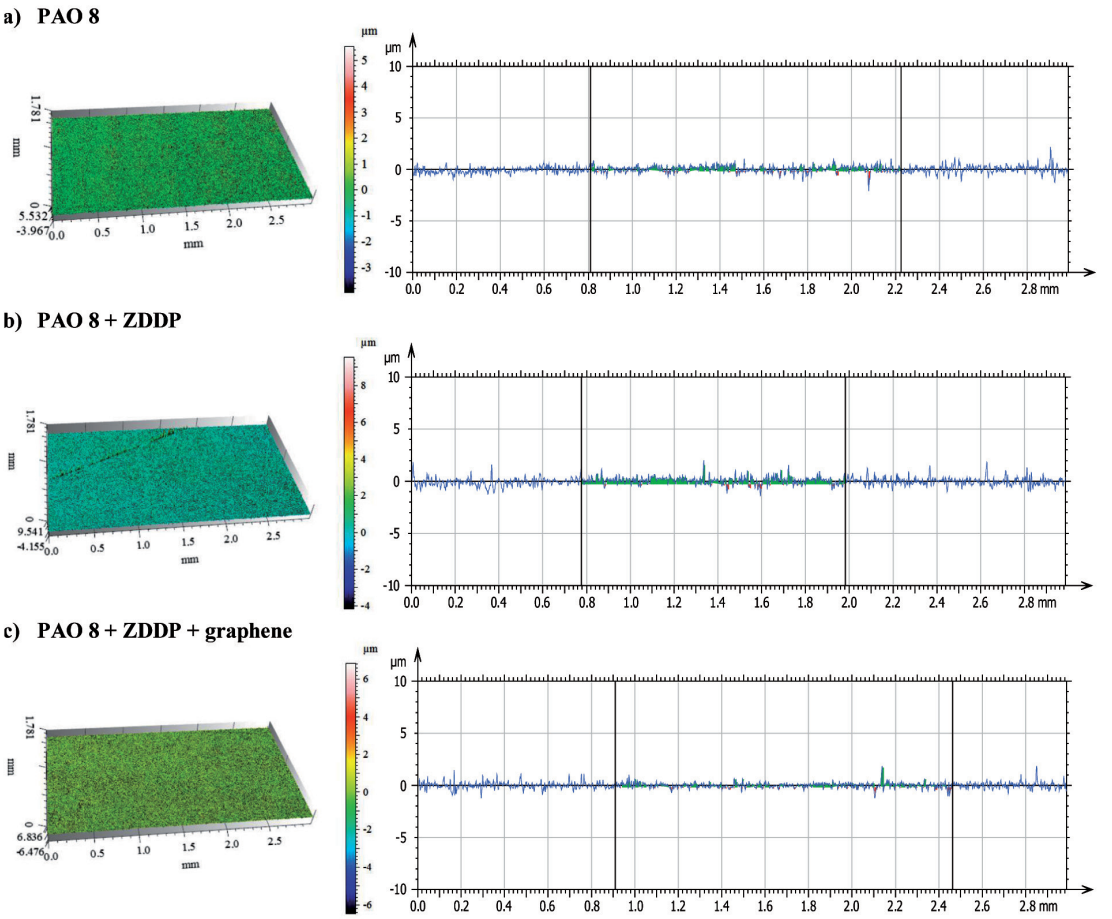

Fig. 5. Isometric views and primary profiles of the discs after the tribological tests after lubrication

Rys. 5. Obrazy izometryczne i profile pierwotne tarcz po badaniach tarciowych w warunkach smarowania

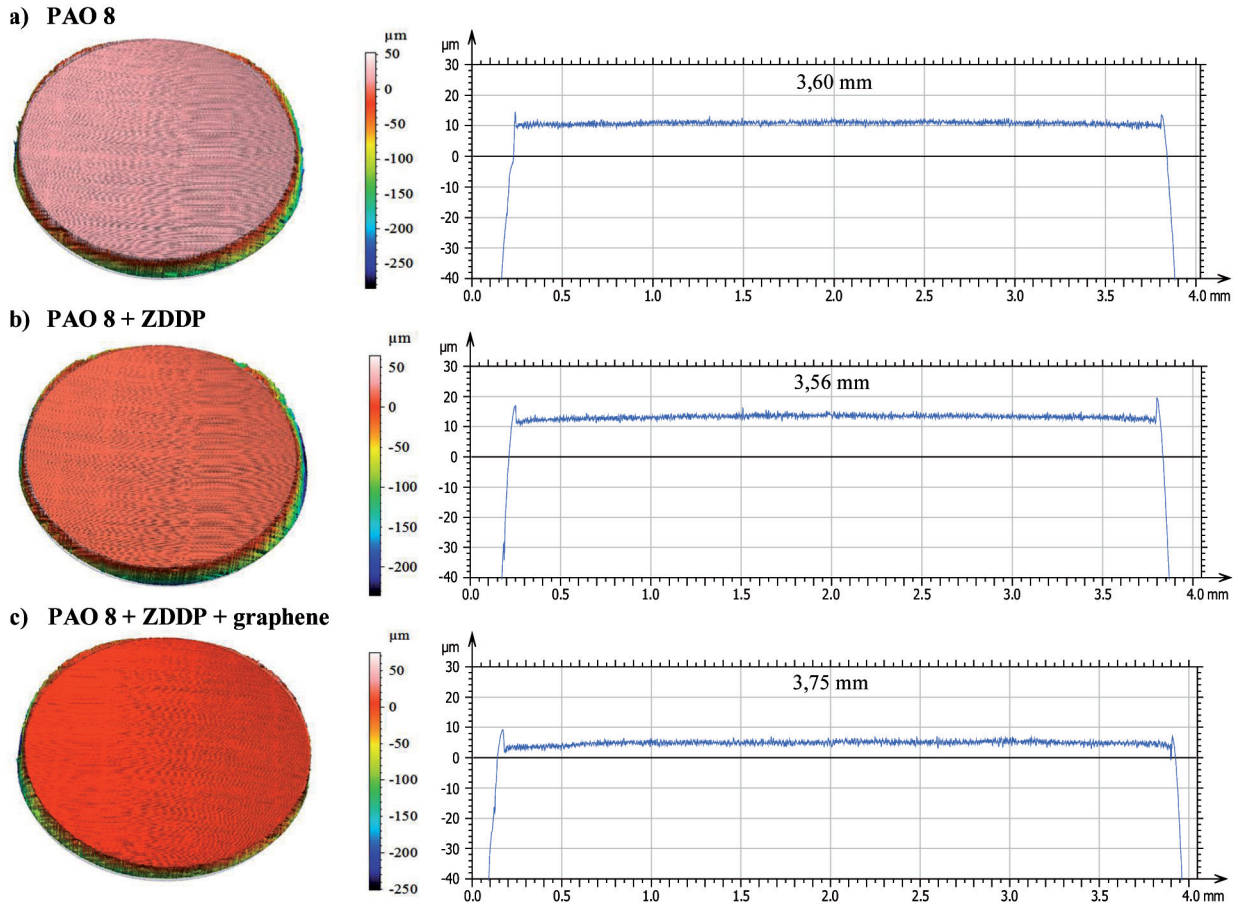

Fig. 6. Isometric views and primary profiles of the balls after the tribological tests after lubrication
Rys. 6. Obrazy izometryczne i profile pierwotne kul po badaniach tarciowych w warunkach smarowania

When analysing the radii and heights of the worn balls after friction tests, the highest values were obtained after friction with PAO 8 + ZDDP + graphene lubrication. The PAO 8 + ZDDP lubricant showed the least wear on the ball.

The surface roughness parameters of the discs and ball before and after the friction tests are summarised in **Table 7**.

Table 7. Surface texture parameters for the discs and balls before and after the tribological tests for PAO 8, PAO 8 + ZDDP and PAO 8 + ZDDP + graphene
Tabela 7. Parametry chropowatości powierzchni dla tarcz i kul przed oraz po testach tribologicznych dla PAO 8, PAO 8 + ZDDP i PAO 8 + ZDDP + grafen

Surface texture parameters	Before test		Past test					
			PAO 8		PAO 8 + ZDDP		PAO 8 + ZDDP + graphene	
	disc	ball	disc	ball	disc	ball	disc	ball
Sa [µm]	0.28	0.63	0.23	0.36	0.24	0.38	0.20	0.41
Sq [µm]	0.37	0.87	0.31	0.46	0.36	0.49	0.29	0.53
Sp [µm]	4.31	11.20	4.30	3.37	9.53	3.62	3.90	6.79
Sv [µm]	3.34	34.08	3.21	3.68	3.73	3.14	4.64	3.74
Sz [µm]	7.64	45.28	7.51	7.05	13.25	6.75	8.54	10.53
Ssk [-]	0.38	-0.46	0.03	0.02	1.51	0.17	-0.33	0.03
Sku [-]	7.91	18.40	6.72	3.46	28.29	3.86	14.58	3.87

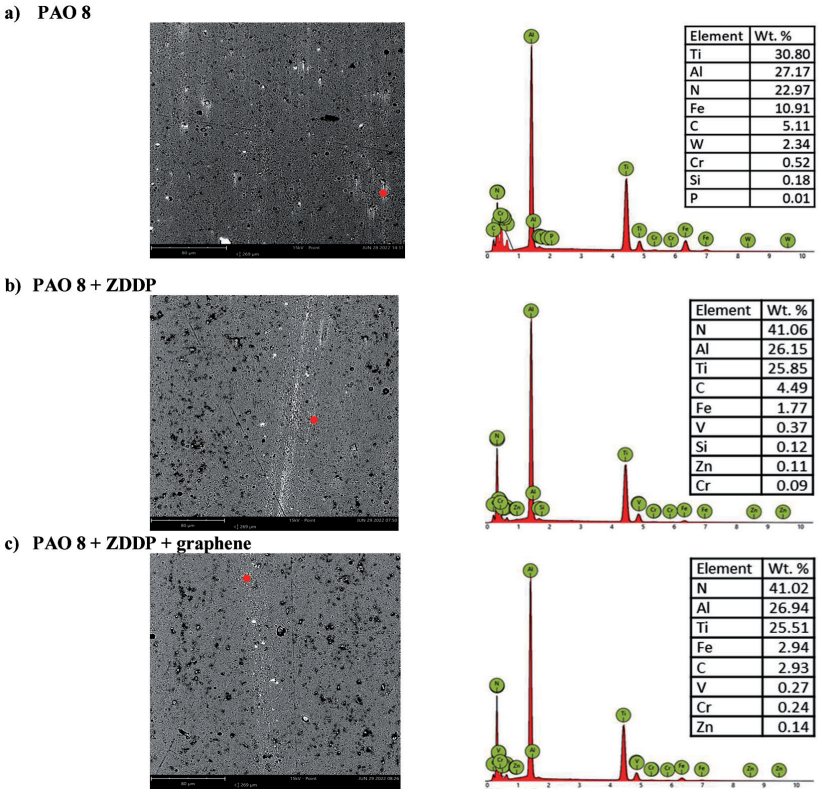

Fig. 7. EDS patterns for different points of the wear track of discs resulting from the sliding contact of the discs with the balls

Rys. 7. Widmo charakterystycznego promieniowania rentgenowskiego z obszaru wytarcia tarcz po kontakcie ślizgowym tarcz z kulkami

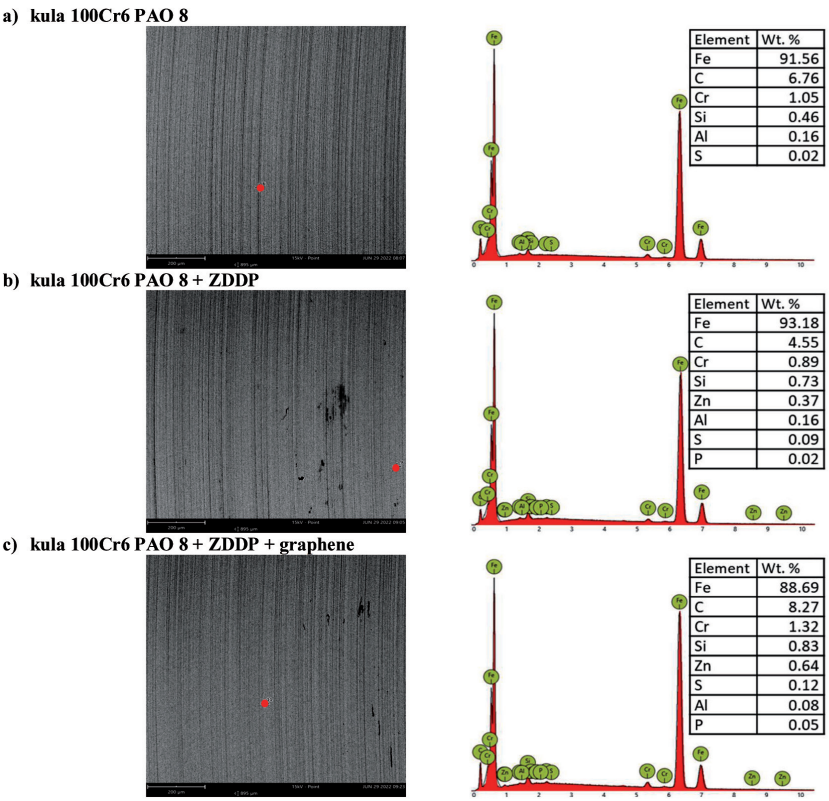

Fig. 8. EDS patterns for different points of the wear track of balls resulting from the sliding contact of the uncoated steel discs with the steel balls

Rys. 8. Widmo charakterystycznego promieniowania rentgenowskiego z obszaru wytarcia kul po kontakcie ślizgowym tarcz stalowych ze stalowymi kulkami

A reduction in the parameter value was observed when comparing the roughness parameters of the discs before and after the tribological tests: Sa, Sq and Sp. A reduction in the parameter value was observed when comparing the roughness parameters of the balls before and after the tribological tests: Sa, Sq, Sp, Sv, Sz and Sku. This shows that the surfaces of the discs and the balls have been smoothed after the friction tests have been performed.

Figure 7 and **8** summarises the results of the chemical composition analysis of the abrasion trace at selected points for the disc (**Fig. 7**) and balls (**Fig. 8**) after tribological tests.

EDS analysis of the abrasion traces showed that after lubricated friction with PAO 8 containing 1.5 wt% ZDDP and 0.005 wt% graphene, the presence of zinc on the surface of the TiAlN-coated disc increased by 21% (**Fig. 7c**) and on the surface of the ball by 42% (**Fig. 8c**) compared to PAO 8 + ZDDP (**Fig. 7b** and **Fig. 8b**). The differences in the amount of zinc on the surfaces after the tribological tests are due to the passivity of the TiAlN coating and the more active surface of the steel counter specimen. Graphene acted as a catalyst, influencing the course of the interaction of a tribocatalytic nature.

CONCLUSIONS

The following conclusions have been drawn from the research carried out.

1. The tribological systems' motional resistance was reduced by adding 1.5% ZDDP and 0.005% graphene to PAO-8 oil. The coefficient of friction value was reduced by 25%.
2. The PAO 8 + ZDDP + graphene lubricant gave the highest linear wear value. This is primarily due to the greater wear of the counter sample, as evidenced by both the wipe mark analysis and the volumetric wear values of the balls. No wear was detected by analysis of the wear marks on the TiAlN coated discs.
3. The synergistic nature of the interactions between ZDDP and graphene was due to their presence in the test lubricant. After friction tests under PAO 8 + ZDDP + graphene lubrication conditions, the highest concentration of zinc atoms was recorded on both the disc and the ball compared to PAO 8 + ZDDP. The graphene acts as a catalyst for the tribocatalytic reaction, resulting in the formation of an anti-wear surface layer.
4. The addition of ZDDP and graphene to the lubricant under test has the effect of a reduction in surface wettability.
5. The results of the friction tests demonstrate the possibility of using the investigated lubricant PAO 8 + ZDDP + graphene as a coolant in machining processes and the TiAlN coating as a cutting tool material for machining steel workpieces. The lubricant used, PAO 8 + ZDDP + graphene, resulted in high ball wear, which is desirable in machining where the workpiece (steel ball) is expected to wear more than the cutting tool (TiAlN coated disc).

REFERENCES

1. Adesina A.Y.: Tribological Behavior of TiN/TiAlN, CrN/TiAlN, and CrAlN/TiAlN Coatings at Elevated Temperature, Journal of Materials Engineering and Performance 31 (8), 2022, pp.6404–6419.
2. Naghashzadeh A.R., Shafyei A., Sourani, F.: Nanoindentation and Tribological Behavior of TiN-TiCN-TiAlN Multi-layer Coatings on AISI D3 Tool Steel, Journal of Materials Engineering and Performance 31 (6), 2022, pp. 4335–4342.
3. Abegunde O.O., Makha M., Machkih K., Ghailane A., Larhlimi H., Samih Y., Alami J.: Comparative Study on the Influence of Reactive Gas Flow Rate on the Growth and Properties of P-Doped TiAlN Coatings Prepared by DcMS and HiPIMS, Journal of Bio- and Tribo-Corrosion 8 (3), 2022, p. 73.

4. Tillmann W., Grisales D., Echavarrí, A.M., Calderón J.A., Gaitan G.B.: Effect of Ag Doping on the Microstructure and Electrochemical Response of TiAlN Coatings Deposited by DCMS/HiPIMS Magnetron Sputtering, Journal of Materials Engineering and Performance 31 (5), 2022, pp. 3811–3825.
5. Aihua L., Jianxin D., Haibing C., Yangyang C., Jun Z.: Friction and Wear Properties of TiN, TiAlN, AlTiN and CrAlN PVD Nitride Coatings, International Journal of Refractory Metals and Hard Materials 31, 2012, pp. 82–88.
6. Fox-Rabinovich G.S., Beake B.D., Endrino J.L., Veldhuis S.C., Parkinson R., Shuster L.S., Migranov M.S.: Effect of Mechanical Properties Measured at Room and Elevated Temperatures on the Wear Resistance of Cutting Tools with TiAlN and AlCrN Coatings, Surface and Coatings Technology 200 (20), 2006, pp. 5738–5742.
7. Olejniczak A., Shostenko A., Truszkowski S., Fall J.: Radiolysis of Synthetic Oils Based on Polyalphaolefins, High Energy Chemistry – HIGH ENERG CHEM-ENGL TR 42, 2008, pp. 92–94.
8. Kowalczyk J., Kulczycki A., Madej M., Ozimina D.: Effect of ZDDP and Fullerenes Added to PAO 8 Lubricant on Tribological Properties of the Surface Layer of Steel Bate Steel and W-DLC Coating, Tribologia 1, 2022, pp. 19–32.
9. Amrita M., Kamesh B., Revuru R.S., Venkataramana V.S.N.: Tribological Behavior of Graphene-Dispersed Emulsifier Cutting Fluid," Journal of The Institution of Engineers (India): Series C 102 (4), 2021, pp. 1091–1097.
10. Madej M.: The Effect of TiN and CrN Interlayers on the Tribological Behavior of DLC Coatings, Wear 317 (1), 2014, pp. 179–187.
11. https://www.Kronosedm.Pl/Stal-Sw7m-1-3343.
12. Kim K.H., Park S.D., Bae Ch.M.: New Approach to the Soaking Condition of 100Cr6 High-Carbon Chromium Bearing Steel, Metals and Materials International 20 (2), 2014, pp. 207–2013.
13. https://www.Alfa-Tech.Com.Pl/Stale-Konstrukcyjne-Stopowe-Stal-Lozyskowa-Lh15.
14. https://www.Oerlikon.Com/Balzers/Pl/Pl/Portfolio/Rozwiazania-Powierzchniowe-Balzers/Powloki-Na-Bazie-Pvd-i-Pacvd/Balinit/Na-Bazie-Tialn/Balinit-Futura-Nano/?Tab=specyfikacja_4.